CHINESE JOURNAL OF PHYSICS VOL. 52, NO. 1-II February 2014

Review

Intensity Clamping During Femtosecond Laser Filamentation

Weiwei Liu*

Institute of Modern Optics, Nankai University,
Key Laboratory of Optical Information Science and Technology,
Ministry of Education, Tianjin 300071, China
(Received August 30, 2013)

The femtosecond laser filamentation is commonly understood as the result of the dynamic balance between optical Kerr effect induced self-focusing and plasma defocusing effect. When the balance of these two processes is achieved, the laser intensity inside filament is not only stabilized along the propagation distance, but also almost invariable with the increase of the input laser energy. This special phenomenon is named intensity clamping. The intensity clamping represents one of the fundamental characteristics of the filamentation phenomenon. It governs the major evolution dynamics of the laser pulse propagation during the filamentation and impacts extensively the applications of the filamentation. This paper summarizes the main research results about the intensity clamping, including current understanding about the underlying mechanism of the intensity clamping, experimental evidences proving the intensity clamping and some recommended approaches to measure the clamped intensity. The paper also introduced some impressive effects brought by the intensity clamping in various applications, such as high stability of the fluorescence signal in remote sensing, beam-cleaning in short pulse production, etc. The effects are in fact in contrary to the common sense about the outcome of nonlinear interaction, which would be unstable under perturbation. Furthermore, the paper presents some methods to increase the clamped intensity inside the filament. At the end, some other effects that may arrest the beam collapse during the filamentation are briefly discussed. These effects mainly include the diffraction, the dispersion and high order Kerr effect.

DOI: 10.6122/CJP.52.465 PACS numbers: 42.65.Jx, 52.35.Mw, 42.25.Bs

I. INTRODUCTION

Femtosecond filamentation is a unique nonlinear optical phenomenon [1–7], during which ultrashort laser pulse could propagate over long distance with high intensity, overcoming nature diffraction and dispersion. Since the laser intensity is high enough, the optical medium will be ionized and a long plasma channel will be left behind the laser pulse. This plasma channel is often referred to as a filament. In condensed matters, the length and the diameter of the filament are about several millimeters and a few micrometers, respectively. While in gas media, such as air, the length of the filament may reach

*Electronic address: liuweiwei@nankai.edu.cn

hundreds of meters and the diameter is in the scale of a hundred micrometer. The suggested application of the filamentation ranges from lightening control, to remote sensing, to pulse compression, to weather control and THz generation, etc.

During the filamentation, plenty optical processes are involved, including dispersion, diffraction, self-focusing, ionization, Raman excitation, self-phase modulation, four wave mixing, Cherenkov radiation, etc. On the other hand, the scales of the space and time are widely spanned in the study of filamentation. For example, in time, the shortest laser pulse duration may reach sub-cycle, while the life time of the plasma channel could extend up to many microseconds. The studied electromagnetic wave frequency also covers broad range from UV, to visible, to IR and to THz. Furthermore, the filamentation can be observed in extensive transparent optical media such as liquids, glasses and gases. Since its application in atmosphere is particularly attractively, the dynamics of the interactions of ultrafast laser with aerosol, dust and turbulence are also important issues in the course of filamentation. All these concerns complicate the research about the filamentation. However, the understanding about the intensity clamping, a profound phenomenon occurs during the filamentation, provides a key to solve these challenges.

It has been widely accepted that the filamentation is mainly induced by two counteracting effects: one causes the contraction of the laser pulse during the propagation, while the other will lead to the diffraction of the beam. When the balance of these two processes is achieved, the laser pulse will neither diffract significantly nor collapse catastrophically, i.e., propagating in a self-guided form. This is the most simplified scenario of the filamentation process. Due to this balance, the laser intensity inside filament is not only stabilized along the propagation distance, but also almost invariable with the increase of the input laser energy. This special phenomenon is named intensity clamping. The intensity clamping represents one of the fundamental characteristics of the filamentation phenomenon and impacts extensively the applications of the filamentation. This paper is then aimed to give a brief review about the important research results about the intensity clamping.

II. PROOF OF INTENSITY CLAMPING

It is well known that the whole filamentation process starts with laser beam self-focusing induced by the intensity dependent refractive index, which is written as $n = n_0 + \Delta n_{kr}$. Here n_0 is the linear index of refraction and $\Delta n_{kr} = n_2 I$, the Kerr nonlinear index of refraction; n_2 and I being the coefficient of Kerr nonlinear index of refraction and the local intensity, respectively. For the self-focusing to occur, the transverse spatial intensity distribution of the pulse across the wavefront should not be uniform. Assuming a Gaussian CW beam, its intensity decreases radially from the center to the edges. Since the phase velocity is given by $c = c_0/n$ where c_0 is the light speed in vacuum, the central part of the beam propagates slower than the rest giving rise to a concave wavefront and the beam self-focuses.

However, different views have been brought forward to interpret the dominant effect balancing the self-focusing. Dated back to 1960s, when the filamentation was experimen-

tally observed as a serial of damage spots inside glasses by using nanosecond laser pulse, the efforts of retrieving the counteracting effect to self-focusing was limited to condensed matters due to the available low laser power. The masking of optical breakdown in condensed matters using long laser pulses however impeded the advancement of the understanding of the 'filament', and restricted the perspective for applications. For example, the role of plasma generation during the formation of the filament has not been extensively taken into account although it had been brought forward by Bloembergen in the early seventies [8, 9]. Owing to the development of the chirped pulse amplification (CPA) technique [10, 11], it has been possible to achieve femtosecond (fs) laser pulses with terawatt (TW) level peak power. Nonlinear phenomena during propagation of such intense ultrashort laser pulses become much more pronounced than for longer pulses. It is not only due to the high peak power, but also because of the short pulse duration that avoids the conventional optical breakdown [12–18], in which case the medium gets totally ionized through collision processes induced by the long pulse. Moreover, the filamentation could be conveniently observed in gas media [19], which normally require a few gigawatts (GW) laser power to exceed the self-focusing critical power. This revealed new attention to the research on the filamentation phenomenon.

The inspiring experiments were carried out to demonstrate the generation of filamentation over several tens of meters by propagating near infrared ($\sim$ 800 nm) fs laser pulses [20–22]. Particularly, the researchers in Michigan University measured the pulse energy inside the generated filament in air. It was performed by reflecting the laser pulse at grazing angle of a glass slide, thereby avoiding the damage to the glass. The obtained results showed that the pulse energy contained inside a filament is roughly constant. They proposed that the defocusing effect of the self-generated plasma during the filamentation was the counteracting effect to balance the self-focusing. Numerical simulation was also performed based on this idea. The laser intensity was found to be clamped as a result of the plasma defocusing effect as shown in Fig. 1.

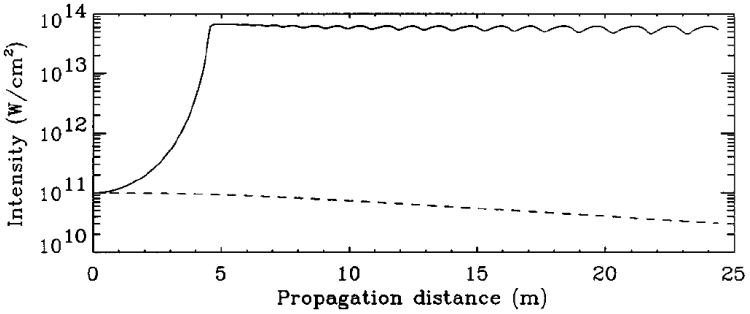

FIG. 1: Calculated intensity during the filamentation (solid line) and the linear propagation (dashed line), respectively. From [20].

In 1998, Brodeur and Chin stated that in order to explain the asymmetry broadening of the supercontinuum spectrum generated by the filamentation in condensed matters, the

contribution of the plasma formation to the refractive index has to been included in the self-phase modulation modeling as summarized in Fig. 2 [23]. They have further found the close correlation between the maximum blue frequency shift of the supercontinuum and the bandgap energy needed for the multiphoton excitation of electrons into the conduction in various condensed matters [24]. The results confirmed the crucial role of the plasma generation in sustaining the filament.

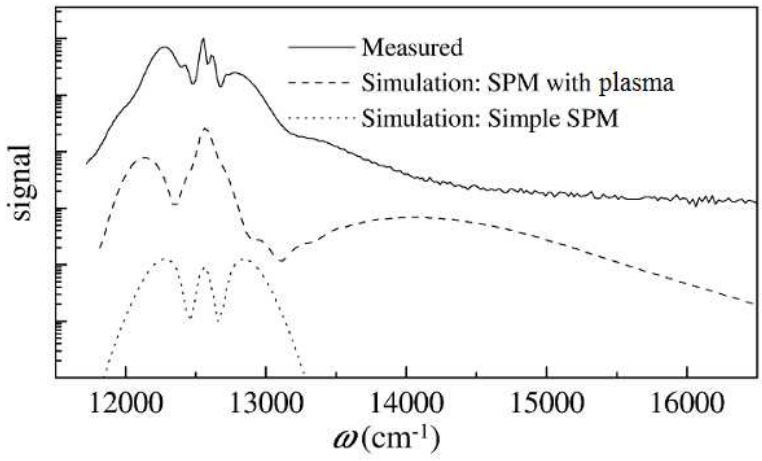

FIG. 2: Supercontinuum spectrum measured during filamentation (solid line) and obtained by numerical simulation with (dashed line) and without (dotted line) taking into account plasmas generation, respectively. From [23].

Since then, the essential role of plasma defocusing that leads to intensity clamping has become a hot topic in the community. It is worth noting that S. L. Chin's group in Laval University has made tremendous contribution to the understanding of the intensity clamping.

Plasma generation takes place as soon as the laser intensity at the self-focus is high enough to generate a significant amount of free electrons in the medium. In fact, the major fundamental physics of filamentation is the same in all optical media, be they gases, liquids or solids. The difference lies in the detail of free electrons generation. In gases, it is tunnel/multiphoton ionization of the gas molecules inside the self-focal volume resulting in the plasma [25]. In condensed matters, it is the excitation of free electrons from the valence to the conduction bands [23] followed by inverse Bremstrahlung and electron impact ionization [2] before the short pulse is over. The well-known type of optical breakdown of the medium (generation of a spark) by longer laser pulses in the picosecond and nanosecond regimes does not occur in the femtosecond self-focusing regime because there is not enough time to sustain cascade (avalanche) ionization. For example, at one atmospheric pressure, the mean free time of electron collision is $\sim$ 1 ps. This time is longer than the fs pulse duration so that only tunnel/multiphoton ionization, an 'instantaneous' electronic transition process, is responsible for the generation of free electrons [25] even if the full pulse is

involved in the self-focusing. In condensed matters, some cascade ionization will contribute to the total number of free electrons. Its contribution strongly depends on the geometrical focusing condition. However, even in the case of extremely strong external focusing, not many cycles of collision can be involved, and it is too little to induce total ionization [21]. That is to say, in both gases and condensed matters, the plasma density induced by femtosecond laser pulses during self-focusing is only a tiny fraction (about 10^{-3}) of the neutral density [23, 26].

Considering the ionization rate in gases when the filamentation takes place, it is generally written as

$$\frac{\partial N_e}{\partial t} = \sigma I^m (N_0 - N_e), \tag{1}$$

where N_e denotes the free electron density inside the filament, σ and I represent the ionization cross section and the laser intensity, respectively. N_0 indicates the neutral molecule density. Because tunnel/multiphoton ionization is a highly nonlinear process and the electron density increases very rapidly with intensity, in Eq. (1) we approximate such an increase as being governed by an effective power law, where m is the effective nonlinear order of ionization. In air, m is about 8 [27]. Because $N_e \ll N_0$, Eq. (1) could be simplified as

$$N_e = N_0 \beta I^m, \tag{2}$$

β is a proportional coefficiency taking into account the cross section and temporal integral. On the other hand, the refraction index change due to the plasma generation can be approximated as

$$\Delta n_p = -\frac{\omega_p^2}{2\omega_0^2} \text{ (ω_0, the central frequency of the pulse)} \tag{3}$$

Here the plasma frequency is given by $\omega_p = \sqrt{\frac{e^2}{\varepsilon_0 m_e} N_e}$, where e and m_e are the charge and mass of the electron, and ε_0 is the permittivity of free space. The effective index of refraction during the filamentation is thus:

$$n = n_0 + \Delta n_{kr} + \Delta n_p = n_0 + n_2 I - \frac{e^2}{2\varepsilon_0 m_e \omega_0^2} N_0 \beta I^m. \tag{4}$$

Qualitatively, it means that the free electron term would quickly catch up with the Kerr term until they are equal; i.e. until $\Delta n_{kr} + \Delta n_p = 0$. At this point, Kerr self-focusing balances free electron defocusing. The laser beam, having now an index of refraction n_0, propagates at the linear speed c. There is no more focusing and the intensity is highest at this balancing point. This is the condition of intensity clamping. That is to say, during self-focusing of a powerful femtosecond laser pulse in an optical medium, there is a maximum intensity that self-focusing can reach. According to the concept of Eq. (2), Kasparian *et al.* has estimated that in air the clamped intensity the filamentation by 800 nm is around 5×10^{13} W/cm^2 [28]. By substituting the wavelength dependent n_2, β and m, the estimated

clamped intensity at 400 nm and 267 nm are 1. 5×10^{13} W/cm^2 and 3×10^{12} W/cm^2, respectively [29].

Soon afterwards, experimental evidences of intensity clamping were demonstrated by S. L. Chin's group. In 2000, Talebpour *et al.* found that the fluorescence spectrum from the excited species inside the filament has little contribution from the plasma continuum and the line broadening was less than that of the spectra radiated from a plasma generated by a long pulse [30, 31]. They concluded that the plasma density does not exceed some limiting value as a result of the defocusing by the electrons resulting from multiphoton ionization and the involvement of high order nonlinearities. Beck *et al.* advanced the work in this direction [32]. As indicated in Fig. 3, they studied the peak intensities of the strongest band heads of two band systems of N_2 fluorescence at 337 nm (open squars) and 391 nm (solid circles) as a function of the input pulse energy. The data were obtained at 0.63 Torr, 400 Torr and atmospheric pressure, respectively.

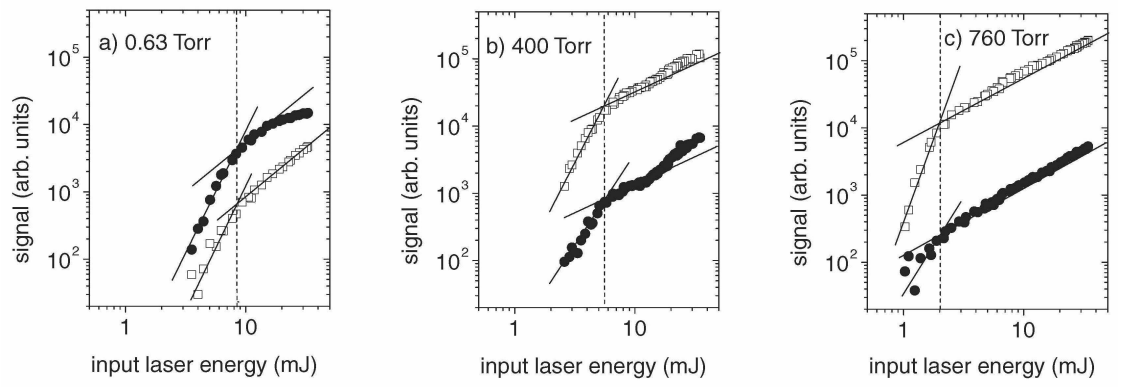

FIG. 3: Nitrogen fluorescence signal as a function of input laser energy at (a) 0.63 Torr, (b) 400 Torr and (c) 760 Torr. From [32].

In Fig. 3, the interpretation of the fluorescence signals as a function of the input laser energy at 0.63 Torr was referred to as the "vacuum case" since it is consistent with the geometrical focusing of the laser pulse without any deformation. The change in its slope in Fig. 3(a) is due to the depletion of neutral molecules in the focal volume. However, the characteristic change in slope of the band head strengths at high pressures (Fig. 3 b, c) occurred at a significantly lower pulse energy than in the "vacuum case". The explanation given is such that the slope changing points at high pressures indeed correspond to the critical power of self-focusing. For higher laser energy, the filamentation takes place and the laser intensity is clamped. Therefore, the fluoresce signal change are mainly associated with the increase of the volume of the plasma column, but not the enhancement of the laser intensity which would give rise to much more steeper slope of the signal increase. Andreas *et al.* also explained the difference of two setting in energies of intensity clamping at 400 Torr and 760 Torr by the pressure dependence of n_2. Since n_2 is proportional to the medium density, the critical power for self-focusing will be inverse proportional to the gas

pressure.

Further experimental evidences of intensity clamping were revealed by Liu *et al.* in condensed matters [33]. In this work, the dependence of the maximum positive frequency shift of the supercontinuum generated by the filamentation on the input laser energy. The results are demonstrated in Fig. 4 by using water as an example. It was found that the maximum frequency shift remains constant at pulse energies that generate single and mutiple filamentation. The constant shift is due to the clamping of the peak intensity inside the filaments. The suggested analyzing procedure is the following.

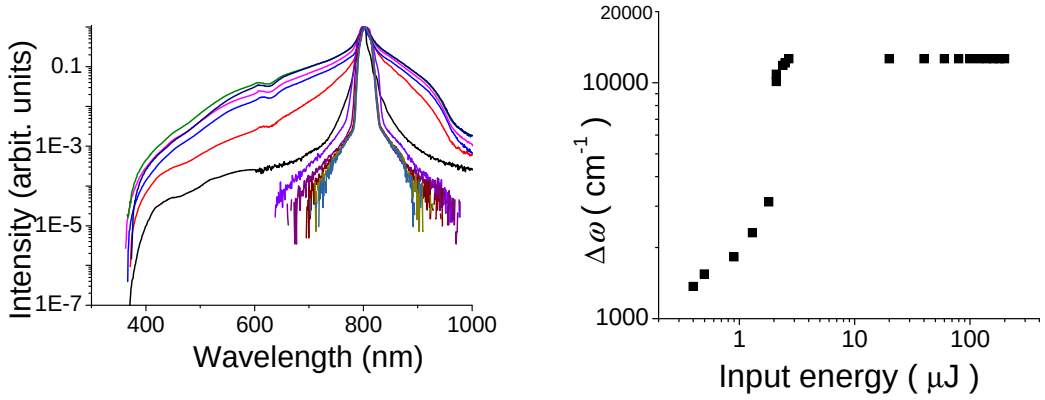

FIG. 4: (a) Supercontinuum spectra as a function of input laser energy during the filamentation in water; (b) maximum anti-stokes frequency shift as a function of the input laser energy. From...

Considering the case of a plane wave, given by the electric field $E(z,t) = E_0 \exp\left(i\left(\omega_0 t - \omega_0 n(z,t) z/c\right)\right)$, propagating in the nonlinear medium, the frequency variation caused by self-phase-modulation can be written as:

$$\Delta\omega\left(z,t\right) = -\frac{\omega_0 z}{c}\frac{\partial n}{\partial t} \tag{5}$$

$$\approx -a\frac{\partial I}{\partial t} + bI^m \text{ (after substituting Eq. (1))} \tag{6}$$

$$= -aI_0\frac{\partial f\left(t\right)}{\partial t} + bI_0^m f^m\left(t\right). \tag{7}$$

I_0 is the peak intensity and $f(t)$ is the temporal shape function. c is the speed of light in vacuum, $z$is the propagation distance in the medium, $a = n_2\omega_0 z/c$ and $b = \frac{e^2}{2\varepsilon_0 m_e \omega_0^2} N_0 \beta$ are positive and independent of time. The first summand in Eq. (7) represents a frequency shift due to the non-linear refractive index n_2 of the material, i.e. the interaction of the light with the bound electrons. If n_2 is positive, lower frequencies, red-shift $\Delta\omega_-$, are created in the leading edge and higher frequencies, blue-shift $\Delta\omega_+$, in the trailing edge of the pulse. The second summand appears due to plasma generation via multiphoton excitation in the condensed matters, i.e. the interaction of the light with free electrons, and causes

a blue-shift of the spectrum only. Note that the two summands have a different power dependence on the peak intensity I_0. Thus, the maximum blue frequency shift is expected to be dominated by the influence of the term arising from the non-linear index of refraction at low intensities and by the plasma contribution at high intensities, i.e. :

$$\Delta\omega_{+,\max} \propto \begin{cases} -I_0 \min_t \left(\partial f(t)/\partial t\right) & : \text{at low peak intensities} \\ I_0^m & : \text{at high peak intensities} \end{cases} \tag{8}$$

where $\min_t(\partial f(t)/\partial t)$ denote the minimum value of the time derivative of the temporal shape function. One would expect according to Eq. (8) that the maximum frequency shift of the supercontinuum spectrum on the blue side is highly sensitive to changes in the peak intensity. Hence, constant frequency shift depict in Fig. 4(b) eventually reveals clamped laser intensity inside filament.

III. MEASURING CLAMPED INTENSITY

Fig. 3 and 4 represents qualitatively interpretation of the intensity clamping. Nevertheless, quantitative characterization of the laser intensity is essential not only for the study of intensity clamping, but also for understanding the underlying dynamic of the filamentation process. Due to the fact that the high laser intensity inside the filament is unsustainable by conventional measuring instruments, precise measurement of the spatio-temporal intensity distribution of the pulse in the course of the propagation is difficult. The interpretation of laser intensity still relies on numerical simulation to a large extent [1–7].

Different methods have been developed to measure the laser intensity inside a filament. In air, it could be roughly estimated by calibrating the grey level of the burn spot left by single-shot pulse on burn paper [34]. Alternative ways of determining the intensity inside a filament are offered by the observation of nonlinear interaction output outside the filament. For example, Lange *et al.* have sent a filamentating pulse into a noble gas cell and through investigating the cut-off frequency of the high order harmonic spectrum generated inside the noble gas cell, a value of 4.5×10^{13} W/cm^2 was obtained for the laser intensity [35].

Another type of means is to make use of Eq. (2). Since β and m are constants for an individual medium and can be obtained in preparation experiment, the free electron density is the key information needed to be known in order to interpret the laser intensity inside the filament. Shadowgraph and holograph are two basic techniques to retrieve the free electron density via the measurement of the refractive index variance [36–38]. For example, Chen *et al.* has measured the free electron density of the filament generated in air and it is several 10^{16} cm^{-3} [39]. In 2005, researchers at SIOM suggested so-called longitudinal diffraction technique to measure the plasma density variable inside a filament [39]. In this scheme, a probe beam was co-axially aligned with the filament. The far field diffraction pattern of the probe beam carried the information of the refractive index spatial distribution. According to Eq. (3), the free electron density is retrieved. In [39], the temporal evolution of the plasma density was even studied by this method. The above introduced methods need

a probe beam. It will complicate the experimental setup and require high quality beam alignment and very stabilized experimental environment.

Some probe-free measurement has been suggested. Liu *et al.* have demonstrated that the measurement of free electron density can be realized by characterizing the Stark broadening of the atomic fluorescence lines associated with the electron impact [40]. This relationship is as simple as:

$$\Delta\lambda_{1/2} = 2\gamma\left(\frac{N_e}{10^{16}}\right), \tag{9}$$

where $\Delta\lambda_{1/2}$ indicates the full width at half maximum (FWHM) of the electron impact broadening induced line width and γ is the electron impact parameter. Therefore, with prior knowledge of the value of γ, one could calculate the electron density from the experimentally obtained line width. This method has been used in argon and air [40, 41]. A representative measurement result obtained for the filamentation in argon gas is shown in Fig. 5. It can be observed that the filament plasma density starts to increase from the distance of 93 cm. It reaches a plateau at 97 cm. The plasma density remains at a level of 6.5×10^{-16} cm^{-3} for 6 cm and begins to decline again from 103 cm. The plateau of the plasma density arises due to the intensity clamping phenomenon. By using the same method, Bernard *et al.* have investigated the clamped laser intensity as a function of the gas pressure [42]. As shown in Fig. 6, the measured free electron density is eventually proportional to the pressure, i.e. the initial neutral gas density. According to Eq. (2), it implies that the ionization probability is constant at different pressures. That is to say that the clamped intensity is independent to the gas pressure once the filamentation occurs. It is easy to understand because the intensity clamping requires $\Delta n_{kr} + \Delta n_p = 0$, and thus

$$n_2 I = \frac{e^2}{2\varepsilon_0 m_e \omega_0^2} N_0 \beta I^m \tag{10}$$

Since the right hand and left hand sides of Eq. (7) are both proportional to the gas density N_0, the laser intensity satisfying Eq. (7) is independent on the gas density. A consequence of this phenomenon in vertical atmospheric propagation is that the filament size (diameter) will become larger and larger as the altitude increases because of the following reason. Since the critical power for self-focussing P_c is inversely proportional to n_2 and since n_2 is proportional to air density, the critical power for self-focussing increases as the pressure at higher altitude decreases. Hence, to obtain self-focussing at higher altitude, the input peak power of the pulse has to increase. But since the intensity is clamped at the value at sea level, the higher peak power of the pulse has to be contained inside a region with a larger diameter than that at sea level.

Xu *et al.* have studied the clamped laser intensity at various input laser peak power up to 1.5 TW [43]. The results are depicted in Fig. 7. In the experiment, three focusing lenses were used. Fig. 7 indicates that the intensity clamping phenomenon exist for TW level laser pumping. Further experiment suggests that even one further raises the input laser peak power by two orders of magnitude, the increase of the laser intensity inside the filament does not exceed 30% [44].

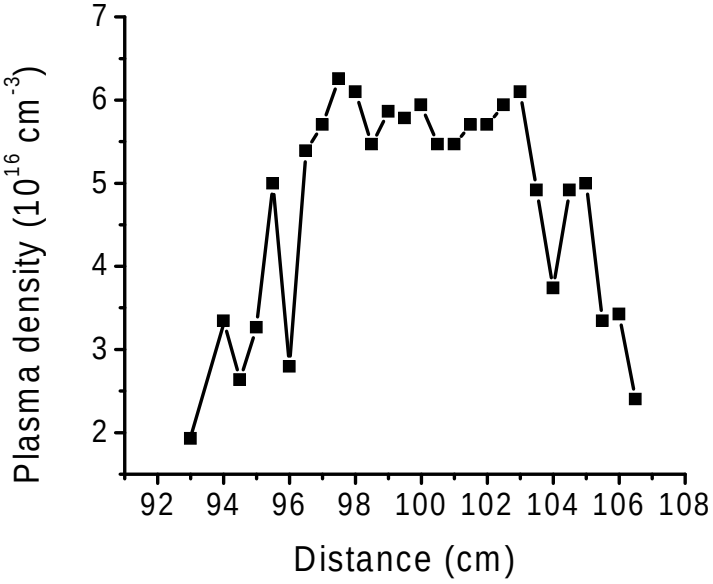

FIG. 5: Measure longitudinal plasma density distribution of a filament generated in air by $f = 100$ cm. From [40].

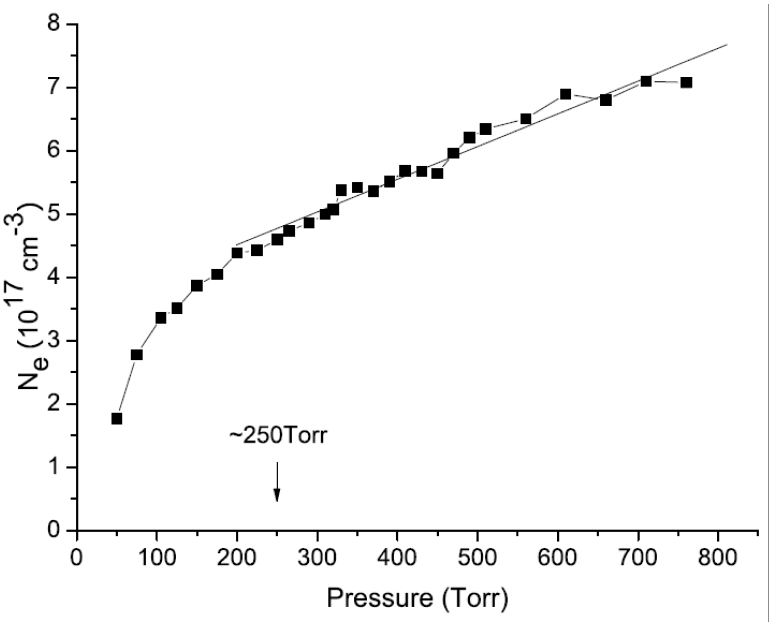

FIG. 6: Free electron density as a function of gas pressure. From [42].

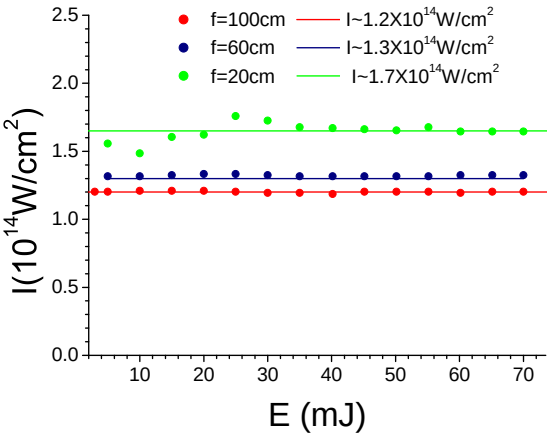

FIG. 7: Measured laser intensity in the course of filamentation in air as a function of the laser energy by using different focusing lenses. From [43].

Recently, Xu *et al.* have suggested another simple way to characterize laser peak intensity inside the filament in air [45]. The central idea is to measure the laser intensity dependent ratio of the signal strength of two nitrogen fluorescence lines, namely, 337 nm and 391 nm, which are assigned to the second positive band of N_2 $\left(C^3\Pi_u \rightarrow B^3\Pi_g\right)$ and the first negative band system of N_2^+ $\left(B^2\Sigma_u^+ \rightarrow X^2\Sigma_g^+\right)$, respectively [10]. Because of distinct excitation mechanisms, the signals of the two fluorescence lines increase with the laser intensity at different orders of nonlinearity. An empirical formula has been deduced according to which laser peak intensity could be simply determined by the fluorescence ratio R of 391 nm and 337 nm:

$$I_0 = 79 \times \left(\frac{2.6}{\mathrm{R}} - 1\right)^{-0.34} \times 10^{12}\ \mathrm{W}\ /\mathrm{cm}^2. \tag{11}$$

According to Eq. (8), the measured laser intensity as a function of the input laser energy is shown in Fig. 8 for difference focal lengths. Fig. 8 indicates that the peak intensity clamps at 4×10^{13} W/cm^2 when $f = 100$ cm. The clamping intensity increases with decreasing of focal length. Eventually, for the shortest focal length we have used ($f = 11$ cm), the clamping intensity is more than 1×10^{14} W/cm^2. The important observation of Fig. 8 is such that the clamped intensity varies with the external focusing condition, which could also be seen in Fig. 7. Similar results have been present by Théberge *et al.* [46]. This has stimulated an approach to increase the laser intensity achieved inside the filament. However, as we will discuss later in this paper, the increase of the laser intensity by this method would not be unlimited.

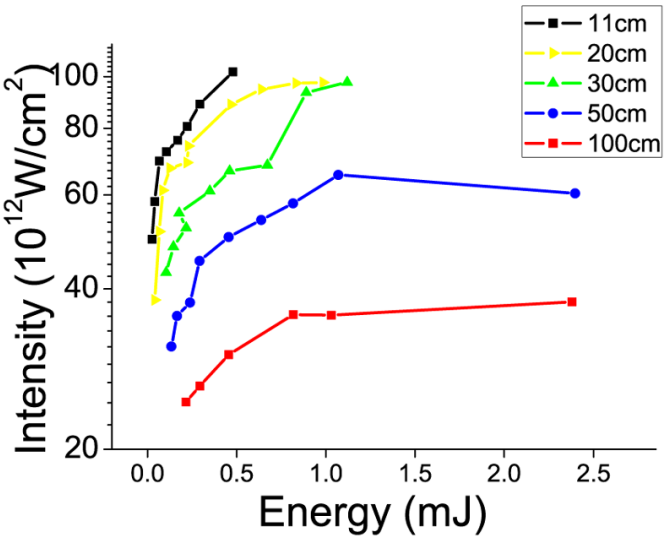

FIG. 8: Measured laser intensity as a function of input laser energy according to Eq. (8) for differenc focusing lenses. From [45].

IV. APPLICATION OF INTENSITY CLAMPING

The impact of the intensity clamping is extensive. From the fundamental physics point of view, because of the intensity clamping, all the laser energy can not be constrained into a single self-focus. Evidences have shown that only about 10% of the total laser energy is embraced inside the filament. The rest laser energy forms broad low intensity robe surrounding the filament. This part of the laser energy forms the background energy reservoir [47–50]. It is important to emphasize that the background is not stationary. The dynamic energy exchange between the reservoir and filament preserves the long distance propagation of the filamentation. Also because of the intensity clamping, when the laser peak power well exceeds the critical power for self-focusing, the laser beam may evolve in the form of multiple re-focusing cycles [51–53], or break up into multiple filaments if perturbation exists in the intensity distribution of the laser beam [1–7]. In conclusion, the intensity clamping governs the major evolution dynamics of the laser pulse propagation during the filamentation.

In application, the most intuitive consequence of the intensity clamping might be the saturation of the outcome from the optical interaction happening inside the filament when the input laser energy keeps increasing. Fig. 3 and 4 are good examples for the obtained fluorescence strength and laser spectrum broadening. Fig. 9 is another example of the output saturation when the intensity clamping is applied in the laser ablation [54]. Fig. 9 illustrates that because of intensity clamping, when the laser peak power is higher than the critical power for self-focusing, further increase of the laser power cannot result in corresponding decrease of the number of the laser shots required to penetrate a metallic

sample. The results hint that the ablation rate will finally approach a stabilized value. Since the saturation point is identical to the critical power of self-focusing, the experimental technique implemented in Fig. 9 could be potentially used to measure the self-focusing critical power and the nonlinear refractive index.

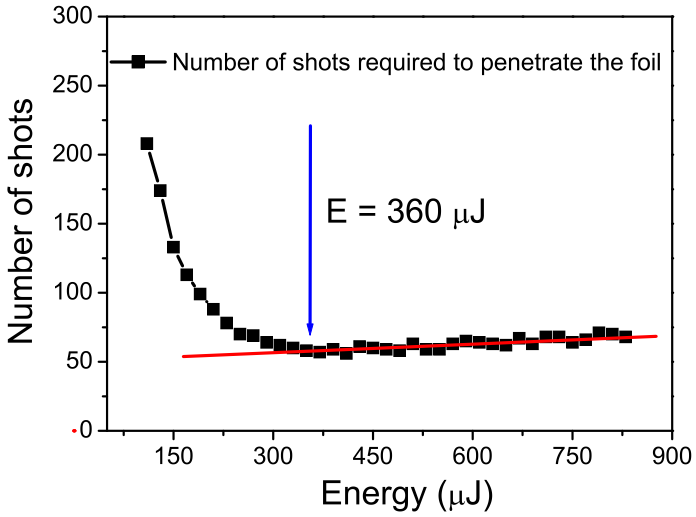

FIG. 9: In air, number of laser pulses required to penetrate the aluminum foil as a function of pulse energy. From [55].

As discussed previously, the intensity clamping leads to the observation that the plasma density is generally only a small fraction of the neutral density during the filamentation. So, the optical radiation emitted from the filament contains little contribution of plasma continuum [30, 33]. Finger-print fluorescence spectra of molecules or atoms are therefore highly distinguishable (see Fig. 10). This clean fluorescence spectrum constitutes the basis of a new material analysis tool – Filament Induced Breakdown Spectroscopy (FIBS) [55]. Since linear diffraction of the laser beam will be overcome by the filamentation, remote detection of fluorescence can be realized. For the sake to demonstrate the application of FIBS, by using a beam sending telescope, filaments have been created at various distances up to 100 m through adjusting the relative distance between the divergent and convergent optical components [56, 57]. In this case, the location of the filament merged with geometrical focus. As displayed in Fig. 11, the recorded back scattered fluorescence signal shows unique invariable feature for distance longer than 30 m [56]. Note that there is a modulation of the result in the range from 60 m to 80 m. It could be explained by the presence of a strong ventilation exit near that region. Evidently, Fig. 11 is opposite to the linear optics principle, according to which the focus intensity is inversely proportional to the square of the focal length. It is due to the profounder phenomenon of intensity clamping

when filamentation occurs.

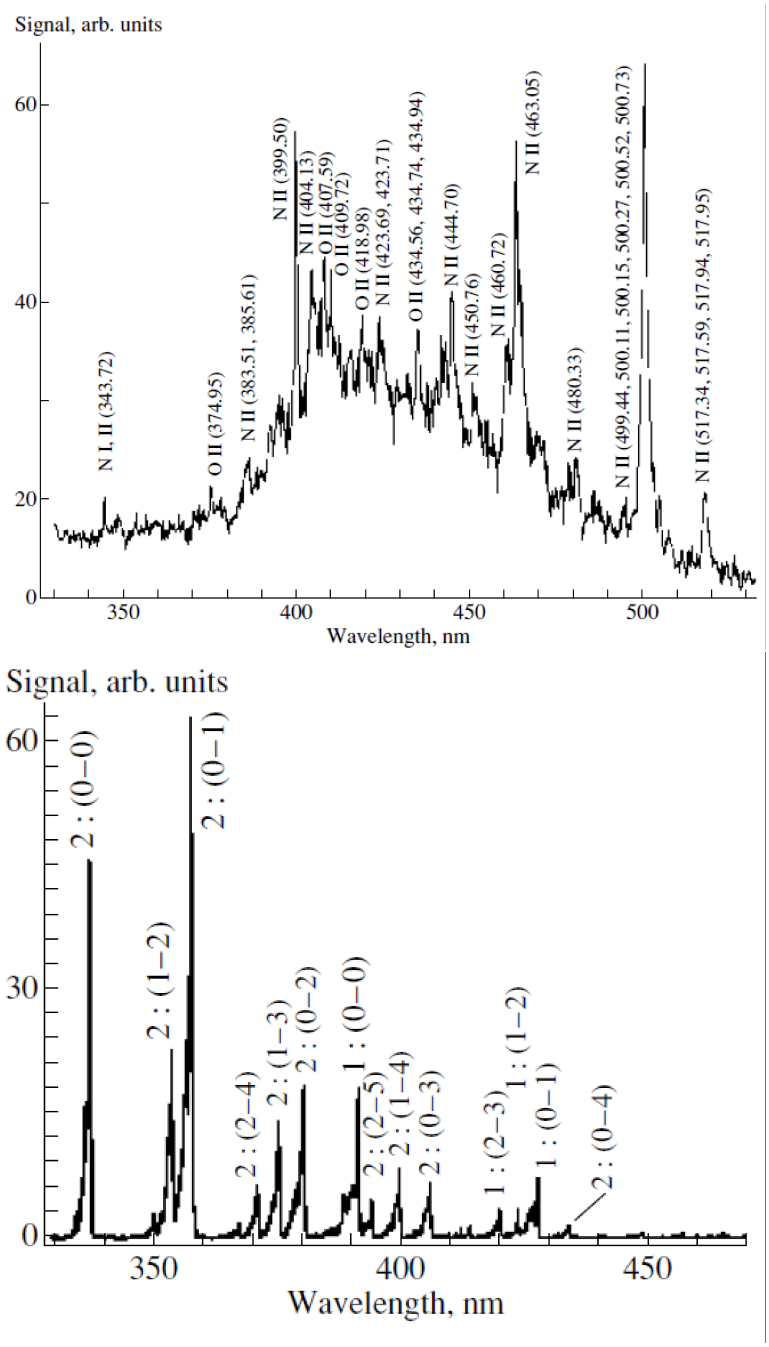

FIG. 10: Spectrum of the optical radiation emitted by (a) breakdown plasma produced by long pulse and (b) a filament in air, respectively. From [31].

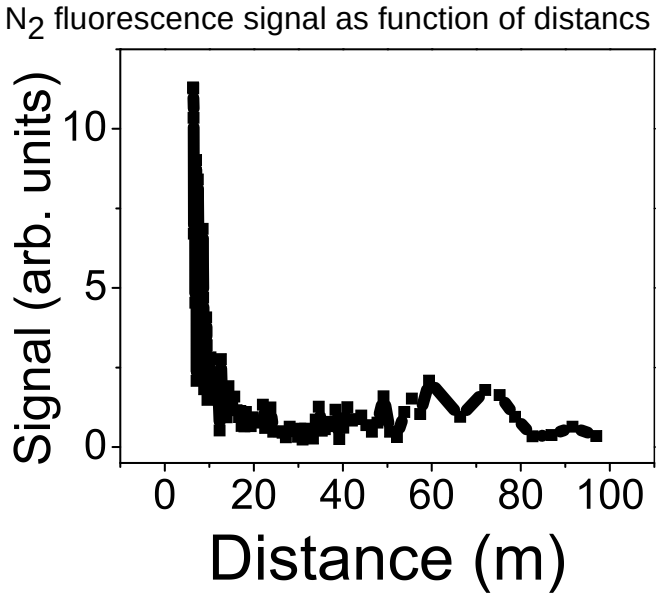

FIG. 11: variation of the nitrogen fluorescence signal in FIBS changes with respect to the location of the filament. From [56].

Another benefit brought by the intensity clamping when applying the FIBS is the high stability of the fluorescence signal. Xu *et al.* have studied the stability of nitrogen fluorescence signal emitted from the filament as a function of propagation distance [57]. The results (Fig. 12) demonstrate that there exists a region where the fluorescence signal is highly stabilized. The measured root-mean-square (RMS) fluctuation of the signal within this range is at least one order of magnitude lower than that of the linear propagation case (dashed line in Fig. 12). With further numerical simulations, they have pointed out that this highly stabilized range is consistent with the intensity clamping zone, where the laser peak intensity is roughly constant. This has established one example of the highly self-stabilized outcome for nonlinear optical interactions taking place inside filament.

More examples of self-stabilized nonlinear interactions could be found in [58]. F. Théberge *et al.* have developed a method to generate tunable and stable few-cycles laser pulses in the visible spectrum by four-wave mixing processduring the filamentation of a near-infrared and an infrared laser pulses in gases ($\omega_{4WM} = 2\omega_{NIR} - \omega_{IR}$) [59]. It is shown experimentally that the intensity clamping occurring inside the filament stabilize the energy fluctuation of the generated tunable pulse (see Fig. 13). This is contrary to the normal wisdom that any non-resonant nonlinear interaction will result in a large fluctuation of the signal/outcome as compared to linear interaction. We call this 'filamentation nonlinear optics'.

In [59], the ultrashort 4WM pulses not only show a remarkable low energy fluctuation, but also possess an excellent mode quality. Fig. 14(a) shows the distorted NIR fluence

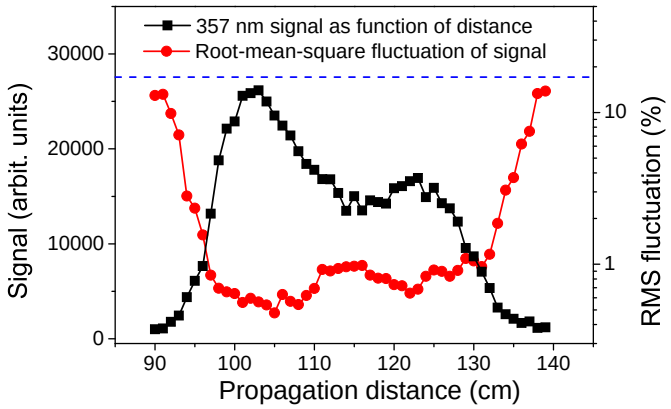

FIG. 12: Black squares (left label): Longitudinal distribution of nitrogen fluorescence signal at 357 nm; red circles (right label): RMS fluctuation of the measured nitrogen fluorescence signal as a function of propagation distance. Blue dashed line: the measured RMS fluctuation by the same detection setup under linear focusing condition. From [57].

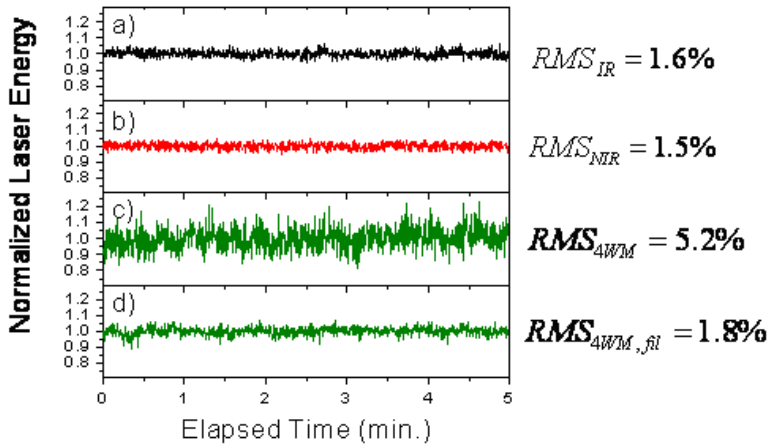

FIG. 13: Time series of energy per pulse normalized over the mean energy for (a) the IR seed, (b) the NIR pulse, (c) the generated 4WM pulse for NIR pump power below the critical power for self-focusing ($P_{NIR} = 0.1P_{cr}$) and (d) the generated 4WM pulse for pump power above the critical power for self-focusing ($P_{NIR} = 2.5P_{cr}$). The root mean square (RMS) energy fluctuations are indicated on the right-hand side for the respective time series. From [59].

distribution before the filament and Fig. 14(b) shows the exceptional beam quality profile of the 4WM pulse generated through filamentation. The 4WM fluence distribution was smooth, centered on the propagation axis and similar to a symmetric Gaussian profile. The

parameters of the 4WM beam diffracting out of the filament are very similar to those of a near diffraction limited Gaussian beam whose M^2 value was measured to be less than 1.01 while the initial quality factor of the NIR beam was $M^2 = 1.3$. The excellent laser profile of the generated 4WM pulse is due to the spatial self-cleaning process occurring in the filament.

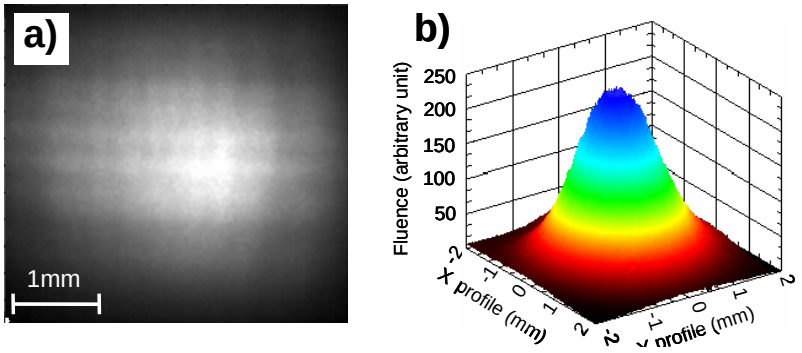

FIG. 14: Distorted NIR fluence distribution used to generate the filament in air and (b) the far-field fluence distribution of the generated 4WM pulse. From [59].

Using a simplified numerical model of the self-focusing process, further light has been shed into the understanding about the physical dynamic of the beam self-cleaning behaviour [60]. As shown in Fig. 15(a), the initial laser beam is Gaussian with ten randomly distributed perturbations added into this smooth beam profile. In Fig. 15, the panel (b)–(d) present the beam profiles at various propagation distances at the pump wavelength of 800 nm. Comparing panels (b)–(c) with (a), one clearly see the continuous shrinking of the beam size due to self-focusing. On further propagation as depicted in Fig. 15(c), the profile of the central zone is evidently improved displaying an excellent beam quality at $z = 33$ cm. It is the manifestation of the self-cleaning behavior of the ultrashort laser pulse filamentation [59, 61]. The plots shown in Fig. 16 are the corresponding intensity distributions along $y = 0$ axis (indicated by white dot lines in Fig. 15). The interesting phenomenon illustrated by Fig. 16 is the gradual spread of the high frequency spatial modulations. The result in Fig. 16 implies that the intensity perturbation contained in the initial beam profile could be treated as high order spatial modes superposing on a fundamental mode. The self-focusing of the laser beam acts as a spatial filter. It focuses the fundamental mode toward the propagation axis, and produces a fundamental mode profile at the self-focus while the higher order modes diffract strongly. Therefore the propagation of higher order modes is mainly governed by the divergence without destroying the high beam quality at the self-focal region. These bring forth the observation of beam profile self-cleaning behavior.

Therefore, if one could sample only the filament core, the output would be very good in quality. This has been confirmed in studying the spatial profile of supercontinuum [60], third harmonic generation in air [58], pulse self-compression [62].

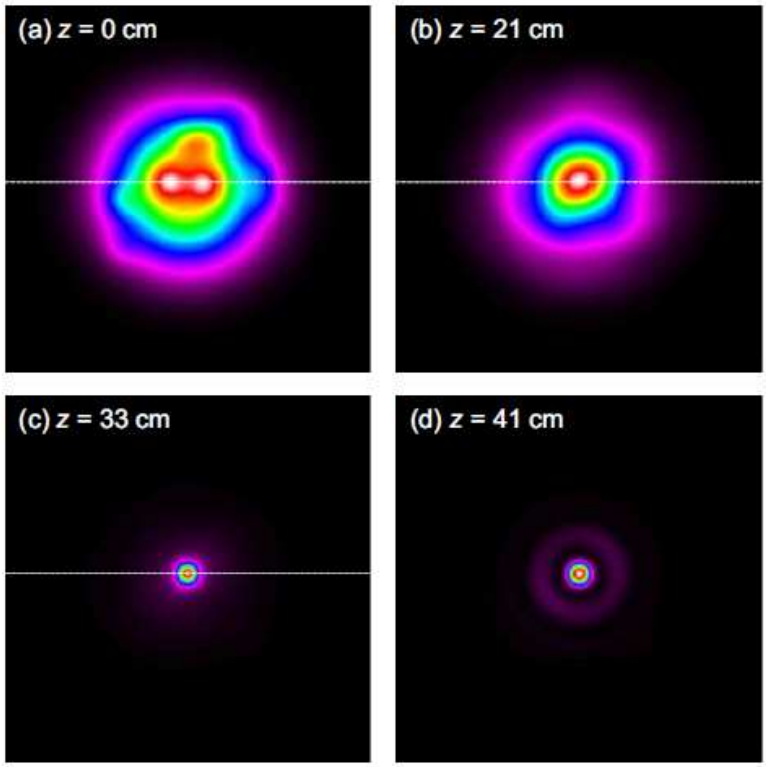

FIG. 15: Numerically simulated laser beam profiles at various propagation distances when the power. From [60].

V. EFFORTS TO INCREASE CLAMPED INTENSITY

So far, we have demonstrated several applications of intensity clamping. In some cases, one may need to increase the laser intensity inside a filament to achieve higher interaction efficiency of optical process.

By the use of the calibrated side imaging technique, Théberge observed that the plasma column parameters and plasma density in the filament are strongly dependent on the external focusing and slightly dependent on the initial laser power as shown [46]. By using the semi-empirical model for the tunnel ionization rate of N_2 and O_2 molecules [14], they estimated from the measured plasma density that the clamped laser intensity inside the filament for the 10 cm focal length lens was 1.6×10^{14} W/cm^2. For the 380 cm focal length lens, this value was 5.3×10^{13} W/cm^2. However, for all the focal lengths explored in the experiment, the peak intensities saturate once the laser power is above the critical power for self-focusing. On the other hand, Kiran *et al.* studied the filamentation process under strong geometric focusing with numerical aperture up to 0.1 [63]. According to the numerical simulation, the peak intensity at the laser focus could be as high as 10^{15} W/cm^2. Liu *et al.* have further pointed out that this value maybe overestimated since double

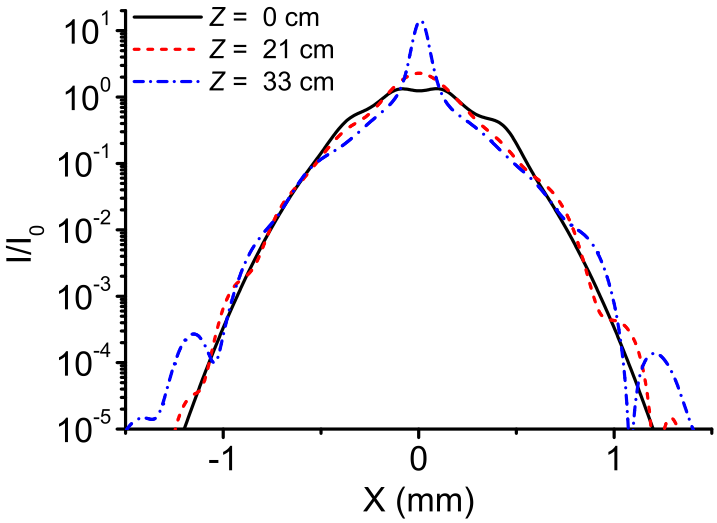

FIG. 16: Intensity distributions along $y = 0$ axis for the panels in Fig. 15. From [60].

ionization might need to be taken into account when the laser intensity exceeds 3×10^{14} W/cm^2 [64]. By considering the double ionization in the analytical model, Liu *et al.* have shown that during the propagation of tightly focused femtosecond laser pulse with numerical aperture of 0.12, the peak intensity is clamped at a level of 5×10^{14} W/cm^2 [64]. Ionin *et al.* have given a research on the influence of external focusing conditions on absolute energetic characteristics of third harmonic, the result shows that the intensity clamping still governs the THG efficiency for different numerical aperture magnitudes at higher laser powers [65]. Although improved peak intensity can be obtained in the filament core by use of tight focusing, under such condition the filament cannot be launched far away.

Another efficient way to change the external focusing is the so-called space-time focusing technique [66]. The laser was dispersed by a parallel pair of 1500 lines/mm gratings in the horizontal direction. It was then focused with a 100 cm focal length lens into the air. They have shown that by employing the spatio-temporal focusing technique, the peak intensity in the filamentation core can be effectively enhanced as compared to that allowed by a loose focusing geometry. In addition, the filamentation length is significantly shortened as a result of elongated pulse duration in the out-of-focus region. This technique could be of great interest in remote sensing for achieving better spatial (longitudinal) resolution and high signal-to-noise ratio while keeping the flexibility of being able to project the filament at long distances as recently experimentally confirmed by Zeng *et al.* at a distance of 22 m away [67]. It can also be useful for other important applications, such as high-order harmonic generation. Higher conversion efficiency and higher cutoff photon energies could be attainable due to the higher achievable peak intensity benefited from the temporal focusing

technique [67].

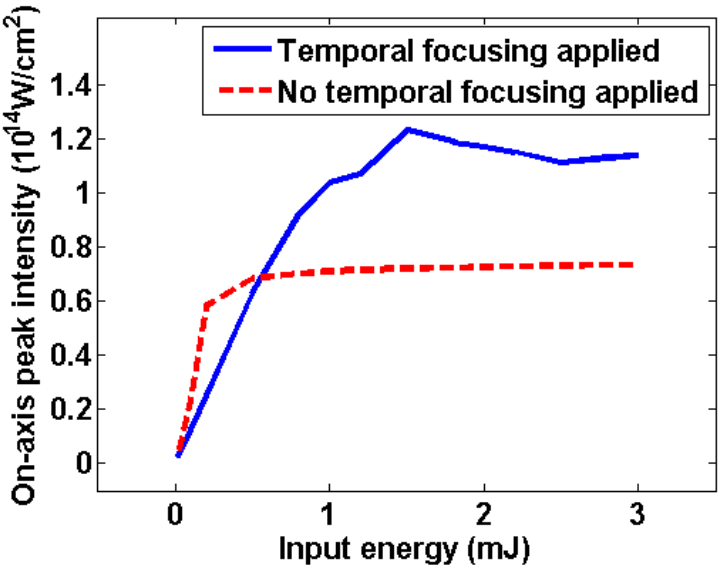

FIG. 17: Simulated clamped laser intensity with (solid line) and without (dashed line) spatio-temporal focusing technique. Form [66].

Lately, researchers have suggested intercrossing two filaments to realize energy coupling between two pulses in nitrogen gas. Kosareva *et al.* have demonstrated that when two filaments cross each other at an angle as small as 0.16°, two filaments merge together [68]. The peak intensity attained in the case of two filaments merging is just 1.3 times higher than that reached in a single filament. Stelmaszczyk *et al.* and Wu *et al.* have reported efficient white light generation in fused silica block and third harmonic generation in argon gas by dual filaments interaction, respectively [69, 70]. In the later work, the incident angle between two filaments is about 0.32°.

Recently, a theoretical work has studied the sub-cycle spatiotemporal dynamics of the laser transformation during filamentation by retaining the full electric-field of the laser pulse. The result predicts a sub-fs intensity spike, having intensity exceeding the clamping intensity by a factor of 3, can last for a short propagation distance in the filamentation process [71]. The theoretical predication has been recently reproduced by Sun *et al.* [72]. The longitudinal distribution of the laser peak intensity inside a half meter long femtosecond laser filament in air was studied by measuring the signal ratio of two nitrogen fluorescence lines, 391 nm and 337 nm. As shown in Fig. 18, the experimental results reveal that laser peak intensity initially remains almost constant ($\sim 4.3 \times 10^{13}$ W/cm^2) inside the filament. However, before the end of the filament, surprisingly the laser intensity undergoes dramatic increase. A maximum intensity as high as 2.8×10^{14} W/cm^2 could be reached. As discussed in [71], the experimentally observed sharp intensity increase shown in Fig. 3 could be attributed to the re-focusing of the reservoir energy at the end of the filament. In this

case, when the inward energy flow to the axis is faster than the energy divergence caused by the plasma due to a shock formation, higher laser intensity could be obtained. It is worth mentioning that the high intensity is only achieved in a very confined spatio-temporal area. For example, in argon gas the duration of the created short pulse could be sub-cycle and the diameter is only a few microns, which is around one order of magnitude less than the diameter within the plateau region [71].

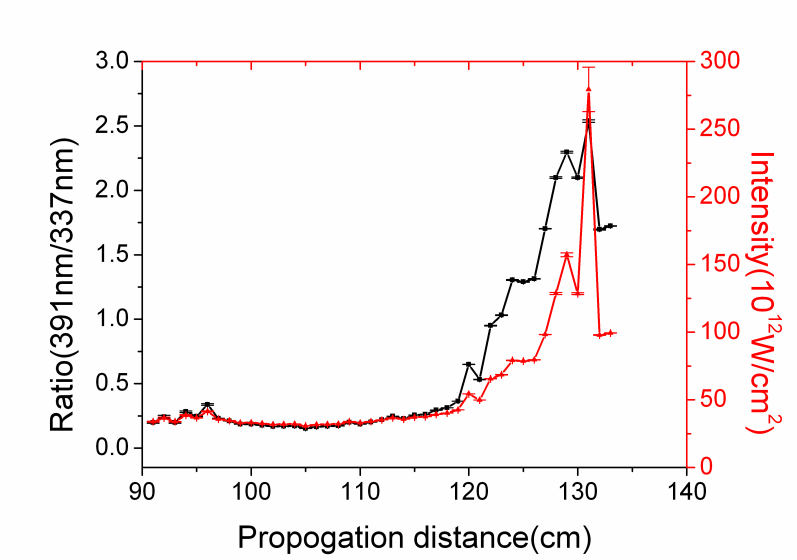

FIG. 18: Evolution of R=S_{391nm}/S_{337nm} versus distance (black line, left label) and the retrieved laser peak intensity according to Eq. (8) (red line, right label). From [72].

VI. OTHER EFFECTS MAY BALANCE SELF-FOCUSING

Up to now, we have considered that the intensity clamping is mainly induced by the dynamic balance between the optical Kerr effect caused self-focusing and the plasma defocusing effect. However, some other scenarios have suggested intensity clamping without ionization. That is to say that the balancing is achieved by effects other than plasma defocusing. These effects include diffraction, dispersion and high order Kerr effect.

In 1960s, Chiao *et al.* proposed the self-trapping model based on a continuum wave (CW) theory [73]. In this model, the natural diffraction was suggested to balance the self-focusing. If the self-focusing effect is not strong enough to counteract the diffraction effect, the consequence is a slowly divergent pulse, slower than that due to pure linear diffraction. When the natural linear diffraction of the pulse is just balanced by self-focusing, a laser beam can produce its own dielectric waveguide and propagate without any change in the beam profile; i.e. the laser beam is self-trapped. Presumably, the filaments are induced by the intense self-trapped beam. The critical balance between the self-focusing

and the natural diffraction is labeled as the so-called critical power for self-focusing [74]. Through the numeric solution of the Maxwell's equations, for a non-paraxial parallel CW Gaussian beam, the critical power for self-focusing is given by: $P_c = \frac{3.77\lambda_0^2}{8\pi n_2 n_0}$ [74], where λ_0 is the laser central wavelength. The critical power in condensed matters is about a few megawatts (MW) and in gas it is a few gigawatts (GW). The definition of critical power shows that it depends only on n_2, n_0 and λ_0 and is independent of the intensity. Subsequently, many investigations on this so-called self-trapped model were carried out with nanosecond (ns) and picosecond (ps) laser pulses in the 1970s. Later, people noticed that self-trapping solutions are not stable. A critical balance between the self-focusing and the natural diffraction is required. Any small perturbation would cause that the self-trapped beam either diffracts or self-focuses.

In 2004, Méchain *et al.* claimed stable non-ionizing channels extending over the distance of kilometers in air [75]. However, the recent researches have shown that the non-ionizing channels are those occurring after the plasma zone where the intensity is still high enough to produce self-focusing, which could balance the linear diffraction and induce the beam to have a very small divergence angle over a long distance as if it is still undergoing filamentation [76–78].

Group velocity dispersion (GVD) has also been suggested to be an effect to arrest the beam collapse due to self-focusing in condensed matters since GVD is much stronger in condensed matters than that in gases [79–81]. In the proposed scheme, the strong GVD in condensed matters may induce pulse splitting and reducing the peak power of the laser pulse during propagation, thus, weakening the self-focusing which is determined by the laser peak power. However, this mechanism is mainly applicable for the laser having lower power than the critical power for self-focusing. When the laser power is higher than the critical power for self-focusing, multiphoton ionization will play more important role than GVD to arrest the beam collapse [82].

In 2004, Kolesik *et al.* have proposed that the filamentation process in water can be interpreted as being due to the propagation of a dynamic nonlinear X waves resulted from the interplay between nonlinearity and chromatic dispersion [83]. Though experimental evidences have shown that the far-field and near-field laser intensity profile share some characteristics of X-wave, detailed numeric study has investigated the influence of these physical effects in the strongly nonlinear regime. The results demonstrated that the group velocity dispersion alone is insufficient to arrest collapse. The collapse is shown to be arrested mainly by plasma generation, but not by dispersion [82].

On the other hand, instead of plasma defocusing effect considered in conventional numerical study of the filamentation process, the high-order Kerr effect (HOKE) has been recently proposed as an alternative mechanism to arrest the self-focusing and inducing the filamentation phenomenon [84, 85]. Though there is still hot debate about the validity of HOKE model [84–86], the plasma generation will take place in both models. The difference lies in the quantities of the outcome parameters, including the plasma density and the filament radius. Particularly, researchers from the University of Arizona have pointed out recently that the well established plasma-defocusing model will give better prediction to

the quantity of the plasma density generated by the filamentation [87].

VII. SUMMARY

In conclusion, though there is still debate about the dominant mechanism inducing femtosecond laser filamentation, the dynamic balance between the optical Kerr effect and the plasma defocusing effect is more accepted as the major reason. The intensity clamping phenomenon is inherently given rise by this balance, leading to an almost invariable laser intensity during the filamentation. Therefore, the intensity clamping represents one of the fundamental characteristics of the filamentation and governs the self-transformation of the laser pulse during the nonlinear propagation. Due to intensity clamping, the output of the nonlinear interaction takes place inside a filament is high stabilized in view of the signal's energy and the spatial mode. This phenomenon has constituted the significant advantages of the filamentation in various applications, ranging from remote sensing, to laser ablation, to self-pulse compression, to laser frequency conversion. Hence, current research focus about the intensity clamping lies on the application of this unique phenomenon, particularly, on the optimization of the clamped laser intensity clamping inside a filament. The main directions include increasing the clamped laser intensity and launch this highly stabilized laser intensity to remote distance. Throughout understanding about the fundamental physics of the intensity clamping will certainly inspire more innovative application and expand the context of the research of femtosecond laser filamentation.

Acknowledgement

This work is financially supported by National Basic Research Program of China (2014CB339802, 2011CB808100), National Natural Science Foundation of China (11174156) and the open research funds of State Key Laboratory of High Field Laser Physics (SIOM).

References

[1] J. Kasparian *et al.*, Science **301**, 61 (2003).
[2] V. P. Kandidov *et al.*, Appl. Phys. B **77**, 149 (2003).
[3] S. L. Chin *et al.*, Can. J. Phys. **83**, 863 (2005).
[4] S. L. Chin, F. Théberge, and W. Liu, Appl. Phys. B **86**, 477 (2007).
[5] A. Couairon and A. Mysyrowicz, Phys. Rep. **441**, 47 (2007).
[6] L. Bergé *et al.*, Rep. Prog. Phys. **70**, 1633 (2007).
[7] J. Kasparian, J.-P. Wolf, Opt. Express **16**, 466 (2008).
[8] E. Yablonovitch, N. Bloembergen, Phys. Rev. Lett. **29**, 907 (1972).
[9] N. Bloembergen, Opt. Commun. **8**, 285 (1973).
[10] D. Strickland, G. Mourou, Opt. Commun. **56**, 219 (1985).
[11] P. Maine *et al.*, IEEE J. of Quant. Electron. **24**, 398 (1988).

[12] A. Talebpour, M. Abdel-Fattah, and S. L. Chin, Opt. Commun. **183**, 479 (2000).
[13] B. L. Fontaine *et al.*, Phys. Plasmas **6**, 1615 (1999).
[14] H. Schillinger, R. Sauerbrey, Appl. Phys. B **68**, 753 (1999).
[15] S. Tzortzakis *et al.*, Opt. Commun. **181**, 123 (2000).
[16] C. Y. Chien *et al.*, Opt. Lett. **25**, 578 (2000).
[17] Q. Sun *et al.*, Opt. Lett. **30**, 320 (2005).
[18] X. Mao, S. S. Mao, and R. E. Russo, Appl. Phys. Lett. **82**, 697 (2003).
[19] P. B. Corkum, C. Rolland, and T. Srinivasan-Rao, Phys. Rev. Lett. **57**, 2268 (1986).
[20] A. Braun *et al.*, Opt. Lett. **20**, 73 (1995).
[21] E. T. J. Nibbering *et al.*, Opt. Lett. **21**, 62 (1996).
[22] A. Brodeur *et al.*, Opt. Lett. **22**, 304 (1997).
[23] A. Brodeur and S. L. Chin, Phys. Rev. Lett. **80**, 4406 (1998).
[24] A. Brodeur and S. L. Chin, JOSA B **16**, 637 (1999).
[25] S. L. Chin, *From Multiphoton to Tunnel Ionization* (Advances in Multiphoton Processes and Spectroscopy), eds. S. H. Lin, A. A. Villaeys, and Y. Fujimura, (World Scientific, Singapore, 2004), p. 249.
[26] S. L. Chin *et al.*, J. Nonlinear Opt. Phys. Mater. **8**, 121 (1999).
[27] A. Talebpour, J. Yang, and S. L. Chin, Opt. Commun. **163**, 29 (1999).
[28] J. Kasparian, R. Sauerbrey, and S. L. Chin, Appl. Phys. B **71**, 877 (2000).
[29] J.-F. Daigle *et al.*, Phys. Rev. A **82**, 023405 (2010).
[30] A. Talebpour, M. Abdel-Fattah, and S. L. Chin, Opt. Commun. **183**, 479 (2000).
[31] A. Talebpour *et al.*, Laser Phys. **11**, 68 (2001).
[32] A Becker *et al.*, Appl. Phys. B **73**, 287 (2001).
[33] W. Liu *et al.*, Opt. Commun. **202**, 189 (2002).
[34] G. Méchain *et al.*, Appl. Phys. B **79**, 379 (2004).
[35] H. R. Lange *et al.*, Phys. Rev. Lett. **81**, 1611 (1998).
[36] H. Yang *et al.*, Phys. Rev. E **66**, 016406 (2002).
[37] Y.-H. Chen *et al.*, Phys. Rev. Lett. **105**, 215005 (2010).
[38] S. Minardi *et al.*, Opt. Lett. **34**, 3020 (2009).
[39] J. S. Liu *et al.*, Phys. Rev. E **72**, 026412 (2005).
[40] W. Liu *et al.*, J. Appl. Phys. **102**, 033111 (2007).
[41] J. Bernhardt *et al.*, Opt. Commun. **281**, 1268 (2008).
[42] J. Bernhardt *et al.*, Appl. Phys. B **91**, 45 (2008).
[43] S. Xu *et al.*, Laser Phys. **22**, 195 (2012).
[44] Z. G. Ji *et al.*, Laser Phys. **20**, 886 (2010).
[45] S. Xu *et al.*, Opt. Express **20**, 299 (2012).
[46] F. Théberge *et al.*, Phys. Rev. E. **74**, 036406 (2006).
[47] A. Dubietis *et al.*, Opt. Lett. **29**, 2893 (2004).
[48] S. Skupin *et al.*, Phys. Rev. Lett. **93**, 023901 (2004).
[49] M. Kolesik and J. V. Moloney, Opt. Lett. **29**, 590 (2004).
[50] W. Liu *et al.*, Opt. Lett. **30**, 2602 (2005).
[51] A. Brodeur *et al.*, Opt. Lett. **22**, 304 (1997).
[52] Z. Wu *et al.*, Opt. Lett. **27**, 448 (2002).
[53] W. Liu *et al.*, Opt. Commun. **225**, 193 (2003).
[54] Z. J. Xu *et al.*, Opt. Express, **16**, 3604 (2008).
[55] H. L. Xu *et al.*, Appl. Phys. B **87**, 151 (2007).
[56] W. Liu *et al.*, Appl. Phys. B **85**, 55 (2006).
[57] S. Xu *et al.*, Opt. Commun. **282**, 4800 (2009).

[58] S. L. Chin, F. Théberge, and W. Liu, Appl. Phys. B. **86**, 477 (2007).
[59] F. Théberge *et al.*, Phys. Rev. Lett. **97**, 023904 (2006).
[60] W. Liu and S. L. Chin, Phys. Rev. A. **76**, 013826 (2007).
[61] B. Prade *et al.*, Opt. Lett. **31**, 2601 (2006).
[62] C. P. Hauri *et al.*, Appl. Phys. B **79**, 673 (2004).
[63] P. P. Kiran *et al.*, Phys. Rev. A. **82**, 013805 (2010).
[64] X. L. Liu *et al.*, Opt Express **18**, 26007 (2010).
[65] A. A. Ionin *et al.*, Laser Phys. **21**, 500 (2011).
[66] B. Zeng *et al.*, Phys. Rev. A **84**, 063819 (2011).
[67] B. Zeng *et al.*, J. Opt. Soc. Am. B **29**, 3226 (2012).
[68] O. G. Kosareva *et al.*, Laser Phys. **19**, 1776 (2009).
[69] K. Stelmaszczyk *et al.*, Phys. Rev. A **79**, 053856 (2009).
[70] H. Wu *et al.*, J. Opt. Soc. Am. B **26**, 645 (2009).
[71] M. B. Gaarde and A. Couairon, Phys. Rev. Lett. **103**, 043901 (2009).
[72] X. Sun *et al.*, Opt. Express **20**, 4790 (2012).
[73] R. Y. Chiao, E. Garmire, and C. H. Townes, Phys. Rev. Lett. **13**, 479 (1964).
[74] J. H. Marburger, Prog. Quant. Electr. **4**, 35 (1975).
[75] G. Méchain *et al.*, Appl. Phys. B. **79**, 379 (2004).
[76] Y. Chen *et al.*, Opt. Lett. **32**, 3477 (2007).
[77] J. F. Daigle *et al.*, Opt. Commun. **284**, 3601 (2011).
[78] Y. Liu *et al.*, Appl. Phys. B, **105**, 825 (2011).
[79] N. A. Zharova, A. G. Litvak, and V. A. Mironov, JETP Lett. **75**, 539 (2002).
[80] G. Fibich and G. C. Papanicolaou, Opt. Lett. **22**, 1379 (1997).
[81] J. E. Rothenberg, Opt. Lett. **17**, 583 (1992).
[82] A. Couairon *et al.*, Phys. Rev. E **73**, 016608 (2006).
[83] M. Kolesik, E. M. Wright, and J. V. Moloney, Phys. Rev. Lett. **92**, 253901 (2004).
[84] P. Béjot *et al.*, Phys. Rev. Lett. **104**, 103903 (2010).
[85] P. Béjot *et al.*, Phys. Rev. Lett. **106**, 243902 (2011).
[86] M. Kolesik, D. Mirell, J.-C. Diels, J. V. Moloney, Opt. Lett. **35**, 3685 (2010).
[87] P. Polynkin *et al.*, Phys. Rev. Lett. **106**, 153902 (2011).